Airflow and teleconnection patterns driving the spatial and temporal variability of high ^{7}Be air concentrations in Europe

M.A. Hernández-Ceballos [a,*], E. Brattich [b], J. Ajtić [c]

[a] Department of Physics, University of Cordoba, Rabanales Campus, 14071, Cordoba, Spain
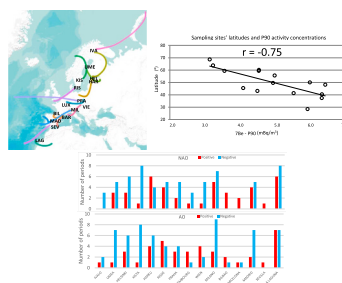[b] Department of Physics and Astronomy "Augusto Righi", Alma Mater Studiorum University of Bologna, via Irnerio 46, 40126, Bologna (BO), Italy
[c] Faculty of Veterinary Medicine, University of Belgrade, Bulevar oslobođenja 18, 11000, Belgrade, Serbia

HIGHLIGHTS

- Evaluate the temporal and spatial variability of the extreme ^{7}Be activity concentrations in Europe (2005–2014).
- Evidence differences in airflow patterns associated with extreme ^{7}Be concentrations in Europe.
- Reveal the influence of the main teleconnection patterns on extreme ^{7}Be concentrations.
- Identify latitudinal differences according to extreme ^{7}Be activity concentrations and meteorological factors.

GRAPHICAL ABSTRACT

ARTICLE INFO

ABSTRACT

The long-term monitoring of the cosmogenic ^{7}Be activity concentrations has been used to better understand the influence of large-scale atmospheric circulation dynamics in the troposphere. With an aim, this study analyzes weekly ^{7}Be data from 15 sampling stations in Europe over 2005–2014. We first define peak (or extremely high) events in each station as those activity concentrations above the 90th percentile, and then investigate their temporal and spatial variability. These events are most frequent in the spring and summer seasons, with a notable latitudinal variability in their number. Next, we use back-trajectory cluster analysis to identify the main advection pathways associated with these high concentrations. To achieve this, persistent periods, i.e., sampling periods over which at least 60% of the calculated backward trajectories arriving at a given site correspond to the same airflow pattern, are taken as reference. This method reveals large differences in the association between the airflow patterns observed at different stations in connection with the ^{7}Be peaks. A comparison between stations shows no clear spatial pattern, which suggests a further influence of mesoscale/local physical processes on the surface ^{7}Be activity concentrations. Finally, the main airflow pattern at each sampling site and the associated ^{7}Be peaks, are related to the main teleconnection patterns of large scale and regional climate variability in Europe: North Atlantic Oscillation, Arctic Oscillation, East Atlantic, East Atlantic/Western Russia, Scandinavian pattern and Western Mediterranean Oscillation. The results point out the connection between the negative phases of NAO and We-MO, and the positive phase of EA with the spatial and temporal variability and occurrence of the ^{7}Be peak activity concentrations. These results show a latitudinal division between northern and southern sites, with similar influence of teleconnection patterns, while those located in the central part of Europe present larger variability in the impact of teleconnection patterns.

---

* Corresponding author.
  E-mail address: f92hecem@uco.es (M.A. Hernández-Ceballos).

1. Introduction

Beryllium-7 (^{7}Be) is a cosmogenic radionuclide widely monitored around the world. For example, there are two databases that include a large number of the ^{7}Be activity concentration measurements in the surface air: the European Radioactivity Monitoring Environmental databank (REMdb) (Sangiorgi et al., 2019), and the International Monitoring System (IMS) developed by the Comprehensive Nuclear-Test-Ban Treaty Organization (CTBTO) (Kusmierczyk-Michulec et al., 2015). One of the reasons for a wide interest in ^{7}Be is its use as a tracer of vertical air mass transport in the troposphere (e.g. Lee et al., 2007) due to its relatively long half-life (53.22 days) and to its production mechanism in the stratosphere (70%) and upper troposphere (30%) (Yoshimori, 2005). At these altitudes, ^{7}Be is produces in spallation reactions between the atmospheric O and N nuclei, and the nucleonic component of the atmospheric cascade induced by galactic cosmic rays (e.g., Dorman, 2004). Hence, the ^{7}Be concentration is at its maximum at around 15–20 km, and decreases towards the surface (Talpos and Cuculeanu, 1997).

Many studies have analysed and described the influence of different factors in the lower atmosphere on the temporal variability of the ^{7}Be activity concentration in the surface layers, such as: vertical exchange between the stratosphere and troposphere (e.g., Huang et al., 2022); dry and wet deposition of the carrier aerosols (e.g., Ioannidou and Papastefanou, 2006); residence times of atmospheric aerosols and latitudinal variability of the ^{7}Be production rates (e.g. McNeary and Baskaran, 2003). A number of studies have also pointed out the influence of synoptic and mesoscale patterns, and hence, the location of the sampling point, on the variability of the ^{7}Be surface concentrations (e.g. Hernandez-Ceballos et al., 2017; Brattich et al., 2017; Ioannidou et al., 2019).

In Europe, several cluster regions, characterised by distinct temporal patterns of the ^{7}Be surface concentrations, have been identified. Specifically, Hernández-Ceballos et al. (2016) identified two main latitudinal groups with a different effect of the tropopause height on the ^{7}Be distribution: northern Europe (50 °N and higher) and southern Europe (south of 50 °N), while Ajtić et al. (2018) noted three distinct regions: north of 55 °N, between 45 °N and 55 °N, and south of 45 °N. These results are explained by the latitudinal impact on the spatial distribution of the ^{7}Be concentrations (e.g., Persson, 2016). However, considering the large area of interest, other factors should also be considered to fully investigate the identified spatial patterns. Since most of ^{7}Be is produced in the stratosphere-upper troposphere layers, its surface concentrations are mainly influenced by: changes in the production rates, which in turn are connected with the variations in the solar activity; changes in the stratosphere-troposphere exchange processes; and horizontal transport through the troposphere.

Our study focuses on the extremely high ^{7}Be activity concentrations recorded at ground level in Europe over 2005–2014. To this purpose, we analysed the 10-year time series of the ^{7}Be activity concentrations in 15 monitoring stations included in the REMdb. We based this comprehensive analysis on the differences and similarities in the advection patterns associated with extremely high ^{7}Be surface activity concentrations, with an aim to establish a relationship between this radionuclide's activity concentrations and the main modes of large scale and regional climate variability: North Atlantic Oscillation (NAO), Arctic Oscillation (AO), East Atlantic (EA), East Atlantic/Western Russia (EA/WR), Scandinavian pattern (SCAND), and Western Mediterranean Oscillation (WeMO). These large-scale teleconnection patterns, which refer to a recurring and persistent, large-scale pattern of pressure and circulation anomalies than span vast geographical areas, are usually defined in terms of the height and/or sea level pressure fields, play a key role in determining meteorological conditions and atmospheric circulations over large geographical areas from days to months (Casado et al., 2008). Indeed, their intensity and position can vary at seasonal, interannual and decadal time scales, and hence they have an impact on atmospheric dispersion,

and hence, on atmospheric surface concentrations of natural or artificial substances. In addition, the regional Western Mediterranean Oscillation (WeMO) teleconnection pattern is also analysed with the purpose to focus on the stations close to the western Mediterranean basin and its vicinities (Martín-Vide and Lopéz Bustins, 2006).

This analysis could further help to:

- Identify areas of common ^{7}Be peaks' behaviour in Europe (in intensity and occurrence).
- Identify airflow patterns related to the ^{7}Be peaks and characterise their temporal and spatial variability.
- Identify the impact of teleconnection patterns on the main airflow patterns influencing extremely high ^{7}Be activity concentrations.

This work is organized as follows. In section 2, we first describe the ^{7}Be dataset and the selection of 15 monitoring sites in Europe, the scheme to calculate backward trajectories, and the cluster method we used. Then, in section 3, we present: 1) the temporal and spatial variability of the extremely high ^{7}Be activity concentrations; 2) the main advection pathways identified by the cluster analysis of back trajectories in each station, and 3) the influence of atmospheric teleconnection indices on the occurrence of most persistent airflow pattern, and so, on high ^{7}Be activity concentrations. We draw the main conclusions in Section 4.

2. Materials and methods

2.1. ^{7}Be activity concentrations

The Radioactivity Environmental Monitoring data bank was created in the aftermath of the Chernobyl accident (1986) by the European Commission (EC) – Directorate-General Joint Research Centre (DG JRC), sited in Ispra, Italy (Sangiorgi et al., 2019). The legal basis behind the REMdb is the Euratom Treaty, Chapter III Health and Safety, Articles 35 and 36 (Council of the European Union, 2016), which clarify that member states shall periodically communicate to the EC information on environmental radioactivity levels. The REMdb has collected data on radionuclide concentrations from the EU member states in both environmental samples and foodstuffs since 1984, and to date, the total number of data records exceeds 5 million, which clearly provides the scientific community with a valuable archive of environmental radioactivity topics.

The ^{7}Be data in the REMdb were supplied by the member states. More information about ^{7}Be sampling can be found in the monitoring report published by the European Commission, which provides information on low levels of radioactivity in the European environment by making use of standardised reporting levels (https://remon.jrc.ec.europa.eu). The activity concentration measurements were performed by the European Union National Competent Authorities and laboratories using gamma spectrometers. However, no tests are conducted by the European Commission to verify the quality and comparability of the ^{7}Be activity concentration measurements delivered by the member states' laboratories. The duration of sampling intervals depended on the location and time period. For the present analysis, we used a set of weekly ^{7}Be measurements, performed between 2005 and 2014, that are stored in the sparse network of the REMdb. Similar to previous studies (Ajtić et al., 2018), the extremely high ^{7}Be activity concentrations in each station were identified using the 90th percentile (P90) for the given station as the threshold concentration. We based our selection of the sampling stations on the number of records higher than or equal to P90 in each individual station (Table 1), thus guaranteeing a large and statistically representative sample.

Fig. 1 and Table 1 show the list of stations and the corresponding information on the number of measurements over the study period (2005–2014). The total number of analysed data points, i.e. with the ^{7}Be activity concentrations above the respective P90 value for the given site,

was 794. Vienna registers the highest number of samples above P90 (57), and we used it to select the other stations, which are those with more than 42 samples above P90 (75% of 57).

2.2. Backward trajectories and cluster analysis

Backward air mass trajectories, initialized at a height of 3000 m above ground level four times a day, at 00, 06, 12, and 18 UTC, with a duration of 96 h, were calculated for each station. The back-trajectory calculations were performed only for those weekly periods that recorded extremely high ^{7}Be activity concentrations. Trajectories were calculated by the Hybrid Single Particle Lagrangian Integrated Trajectory (HYSPLIT) model, developed by the NOAA's Air Resources Laboratory (ARL) (Stein et al., 2015), using GDAS meteorological files. These files include the vertical wind component information, which allows to calculate kinematic three dimensional back trajectories.

The selection of a four-day (96 h) temporal coverage was based on previous works (e.g., Cristofanelli et al., 2006), indicating that air parcels originating in the stratosphere may reach the surface within 5 days. This finding was in agreement with the results of Hernández-Ceballos et al. (2016) observing that the maximum correlation coefficient between the ^{7}Be concentrations and tropopause height is reached within 3 or more days. The back-trajectories were initialized at 3000 m height, which can be considered as representative of the main synoptic transport of the lower troposphere.

For each station, we further applied the cluster method implemented in the HYSPLIT model to group the calculated trajectories according to their length and curvature. This is a bottom-up merging algorithm in hierarchical clustering, and its specific details can be consulted in Stunder (1996) and Rolph et al. (2017). Thus, we obtained an estimation of the general airflow patterns associated with the extremely high ^{7}Be activity concentrations for each station over the whole period of the analysis.

2.3. Sunspots

We used daily data of the number of sunspots retrieved from the Sunspot Index and the Long-term Solar Observations data center (SILSO data/image, Royal Observatory of Belgium, Brussels) (http://www.sidc.be/silso/datafiles).

2.4. Teleconnection patterns

The teleconnection patterns taken in the present study to analyse the ^{7}Be peak activity concentrations account for the main large scale temporal variability of the European region: North Atlantic Oscillation (NAO), East Atlantic (EA), East Atlantic/West Russia (EA/WR), Scandinavian pattern (SCAND), and Arctic Oscillation (AO). The monthly time series of each teleconnection index were obtained from the National Oceanic and Atmospheric Administration's (NOAA) Climate Prediction Center (https://www.cpc.ncep.noaa.gov/data/teledoc/telecontents.shtml). In addition, the monthly time series of the regional Western Mediterranean Oscillation (WeMO) teleconnection pattern was obtained from the Group of Climatology of the University of Barcelona (http://www.ub.edu/gc/wemo/).

3. Results and discussion

3.1. Spatial and temporal distribution of ^{7}Be peaks

During the sampling period and considering all sampling sites, the average of the fifteen calculated P90 activity concentrations was 4.80 ± 0.12 mBq/m^3, where the uncertainty is provided as the mean standard deviation ($Sx/N^{1/2}$, where Sx is the standard deviation and N is the number of sampling sites). From here on, the ^{7}Be activity concentrations and the results obtained refer to those above the corresponding P90 in each sampling site (Table 1).

Fig. 2 shows the annual average of the ^{7}Be activity concentrations in the air considering all sampling sites together with sunspot number observed from 2005 to 2014. This period comprises the end of the 23rd (1996 May – 2008 January) and the middle part of the 24th (2008 January – 2019 December) solar cycles. The maximum concentration was 5.4 mBq/m^3 in 2006, while the minimum value of 4.1 mBq/m^3 was registered in 2013. This figure displays the well-known opposite evolution (e.g., Steinmann et al., 2013) of the solar activity and the ^{7}Be activity concentrations. The correlation between the two parameters is highly negative ($r = -0.83$, at 0.05 significance level).

The maximum value of P90 activity concentration was registered in Madrid and Vienna (6.4 mBq/m^3), and the minimum in Ivalo (3.1 mBq/m^3) (Table 1), an observation which highlights the latitudinal effect on the ^{7}Be surface concentrations (Ajtić et al., 2017). This relationship can be readily observed in Fig. 3, where a high negative correlation between latitude and P90 activity concentrations ($r = -0.75$, at 0.05 significance level) is shown. However, and at the same time, the fact that similar P90 activity concentrations were obtained for sampling stations located at significantly different latitudes, such as Prague and Seville (Table 1), points out the need to consider a combined influence of synoptic and local factors, such as the development of mesoscale-local transport and deposition processes at each specific location to better understand the occurrence of these ^{7}Be events.

Fig. 4 shows the seasonal variability in the occurrence of the extremely high ^{7}Be activity concentrations. This figure points out the similar seasonal pattern observed at all stations, with an increase in spring and summer and a decrease in winter and autumn. This seasonal

Table 1

Sampling sites (latitude, longitude and altitude), total number of weekly samples, the corresponding 90th percentile, and number of samples higher or equal to this value over 2005–2014.

	Latitude (ºN)	Longitude (ºE)	Altitude (m a.s.l)	Total number of samples	P90 (mBq/m^3)	Number of samples ≥ P90
Ivalo (IVA)	68.64	27.57	130.06	477	3.1	52
Umeå (UME)	63.85	20.34	45.18	488	3.2	51
Helsinki (HEL)	60.21	25.06	12.06	488	4.5	52
Kista (KIS)	59.40	17.93	16.94	407	4.4	45
Harku (HAR)	59.39	24.58	36.35	514	3.6	56
Risø (RIS)	55.69	12.10	9.75	506	5.0	51
Prague (PRA)	50.09	14.42	202.56	526	6.0	56
Luxembourg (LUX)	49.63	6.13	280.19	498	5.0	50
Vienna (VIE)	48.22	16.35	193.04	522	6.4	57
Milan (MIL)	45.47	9.18	125.17	423	4.1	45
Bilbao (BIL)	43.17	−2.94	380.72	501	4.5	51
Barcelona (BAR)	41.38	2.12	52.44	511	5.5	54
Madrid (MAD)	40.45	−3.69	715.36	501	6.4	53
Seville (SEV)	37.39	−6.01	8.92	505	6.3	54
La Laguna (LAG)	28.46	−16.29	358.81	517	5.9	56

Fig. 1. Study area and location of sampling stations.

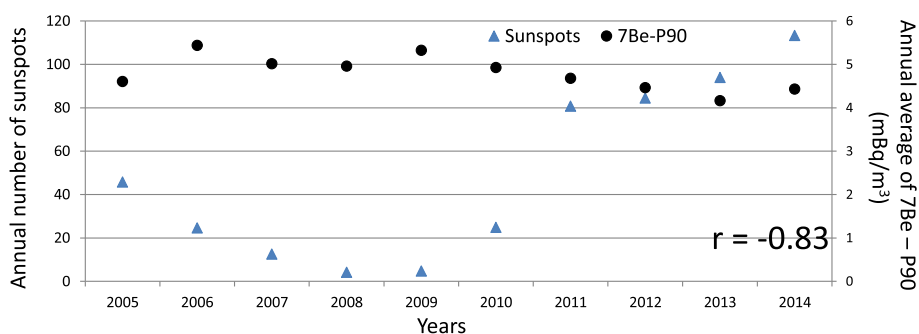**Fig. 2.** Yearly variation in the average of [7]Be P90 activity concentration and sunspot number from 2005 to 2014.

behaviour agrees with the seasonal patterns of the [7]Be activity concentrations previously discussed (e.g., Bourcier et al., 2011; Lozano et al., 2011; Ajtić et al., 2017), and explained by the enhanced vertical transport from the upper troposphere resulting from the intense convective motions typical of the warm season. The seasonal distribution of these extreme periods ranges from 21% to 0% in winter, from 44% to 11% in spring, from 67% to 34% in summer, and from 27% to 6% in autumn. At all sites, the maximum values are more concentrated in the warm (spring and summer) season (from April to August, with the maximum in July). The maximum is registered in Seville (7.9 mBq/m^3). The maximum monthly average of [7]Be over the whole set of stations was

registered in July (6.41 mBq/m^3) and the minimum in December (3.77 mBq/m^3). A clear negative correlation between latitude and the monthly P90 maximum was observed, equal to −0.67. This result confirms the latitudinal influence on the [7]Be activity concentrations, but at the same time suggests again that other factors, such as the local atmospheric conditions, drive the temporal distribution at a given station.

It is interesting to note that the occurrence of peaks is noticeable both in northern latitudes, in agreement with previous studies (Ajtić et al., 2018), and in southern stations (Barcelona, Seville and La Laguna). Hernandez et al. (2008) identified several events of high [7]Be activity concentrations in the Island of Tenerife particularly during autumn and
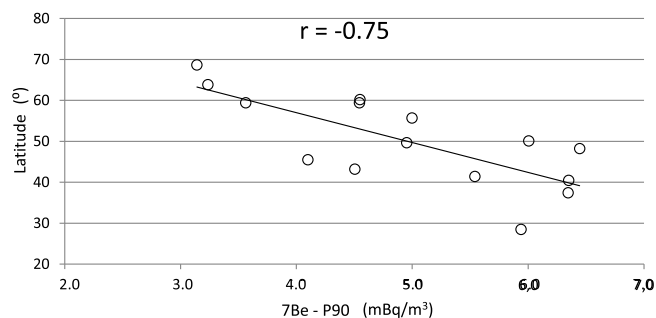
Fig. 3. Relation between the sampling sites' latitudes and P90 activity concentrations.

winter season, which are mainly caused by downward transport of ^{7}Be from the mid-troposphere at mid-latitudes, and Hernández-Ceballos et al. (2016) identified winter ^{7}Be events in Seville associated with the omega synoptic blocking configuration extending either over western Russia and Scandinavia or into the Atlantic Ocean, forcing the prevailing jet stream to the south of Spain respectively with subsequent subsidence.

3.2. Airflow patterns associated with the extremely high ^{7}Be activity concentrations

Fig. 5 shows the centroids of the major advection patterns of the clusters obtained at 3000 m a.s.l. at the 15 sites and the relative percentage frequency of each pattern over the 2005–2014 period. The average number of clusters is 6, with the maximum of 9 registered in Kista, while the minimum of 4 is observed in Risø, Milano and La Laguna. There is no clear relationship between the number of clusters and latitude of the stations ($r = 0.06$). Fig. 5 suggests airflow patterns coming from the west primarily affect the ^{7}Be peak events; however, there is a large variability in the number of airflow patterns and frequencies, which point out differences in the synoptic patterns associated with these events.

To establish an association between the airflow patterns and ^{7}Be peaks, we followed the methodology of Brattich et al. (2017) and looked into "persistent sampling periods"–a specific airflow pattern is attributed to a sampling period only if at least 60% of the calculated trajectories ending at a given site over the sampling period correspond to that advection pattern. Applying this criterion resulted in 231 persistent periods (29%) out of 794 sampling periods. The maximum number of persistent periods was 32 and was registered in Helsinki, while the minimum of only 1 was recorded in Seville. Again, this large variability in the number of persistent sampling periods among stations is not explained by the station latitude, which shows a low correlation

coefficient ($r = 0.2$).

To assess the influence that persistent airflows exert on the high ^{7}Be peak activity concentrations, and to check the validity of working with them, we looked into two different average ^{7}Be concentrations: 1) the mean of all the ^{7}Be peaks (all the values higher or equal P90), and 2) the mean of only the ^{7}Be peaks in persistent sampling periods (the values higher or equal P90 that occurred over persistent sampling periods) (Fig. 6). There are small differences between both P90 means in most of the locations. On average, persistent periods led to an increase in extremely high ^{7}Be activity concentrations of 4.2% (percent variation), and, on the other hand, they corresponded to decreases of 7.0% (percent variation). In this sense, it is necessary to point out how a decrease in P90 during persistent periods is only observed at four stations (Ivalo, Umeå, Harku and Risø), all located in the north of Europe, while the maximum increase is registered in Seville, which is located in the south. A possible explanation for this different behaviour can be associated with the location of the sampling sites and the different impact of synoptic and regional atmospheric systems on the development and occurrence of stratospheric–tropospheric transport (STT) causing high ^{7}Be activity concentrations. In the north, different studies have reported the influence of rapid atmospheric processes on the ^{7}Be activity concentrations, such as the Sudden Stratospheric Warming (SSW) events, which play an important role in the troposphere-stratosphere-mesosphere coupling process and have been previously and positively correlated with the ^{7}Be peak events at high-latitude stations (Pacini et al., 2015; Terzi and Kalinowski, 2017; Ajtić et al., 2018; Brattich et al., 2021). In the south, the omega block configuration at high latitudes combined with the presence of the Azores high pressure system to the west of the Iberian Peninsula can cause subsidence processes associated with high ^{7}Be activity concentrations (Hernandez-Ceballos et al., 2017). Despite these differences, there is a high correlation ($r = 0.97$, at 0.05 significance level), which confirms that the 231 persistent periods can be considered representative in analysing the relationship and influence of airflow patterns on the ^{7}Be peaks.

The seasonal variation of persistent periods in each station indicates that 106 periods (46%) are registered in summer, only 25 in autumn (11%), and 27 in winter (12%), while 73 are identified in spring (31%): this result clearly suggests the seasonal distribution of these periods and, so, of different synoptic conditions associated during the cold (autumn/winter) and warm (spring/summer) seasons. In 60% of the stations, the highest occurrence of the persistent periods is in summer, while there is only one station (Ivalo) showing it in winter.

Once the persistent periods are identified, the purpose of the following analyses is to investigate the dominant airflow pattern linked with the occurrence of ^{7}Be peak activity concentrations at each sampling site. Fig. 7 displays the distribution of persistent periods at each station by clusters. To facilitate the comparison, the X-axis gives the maximum
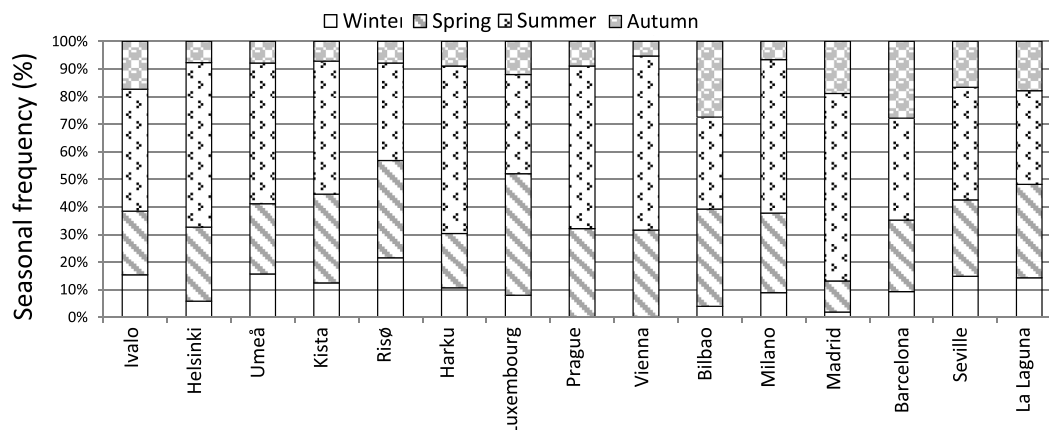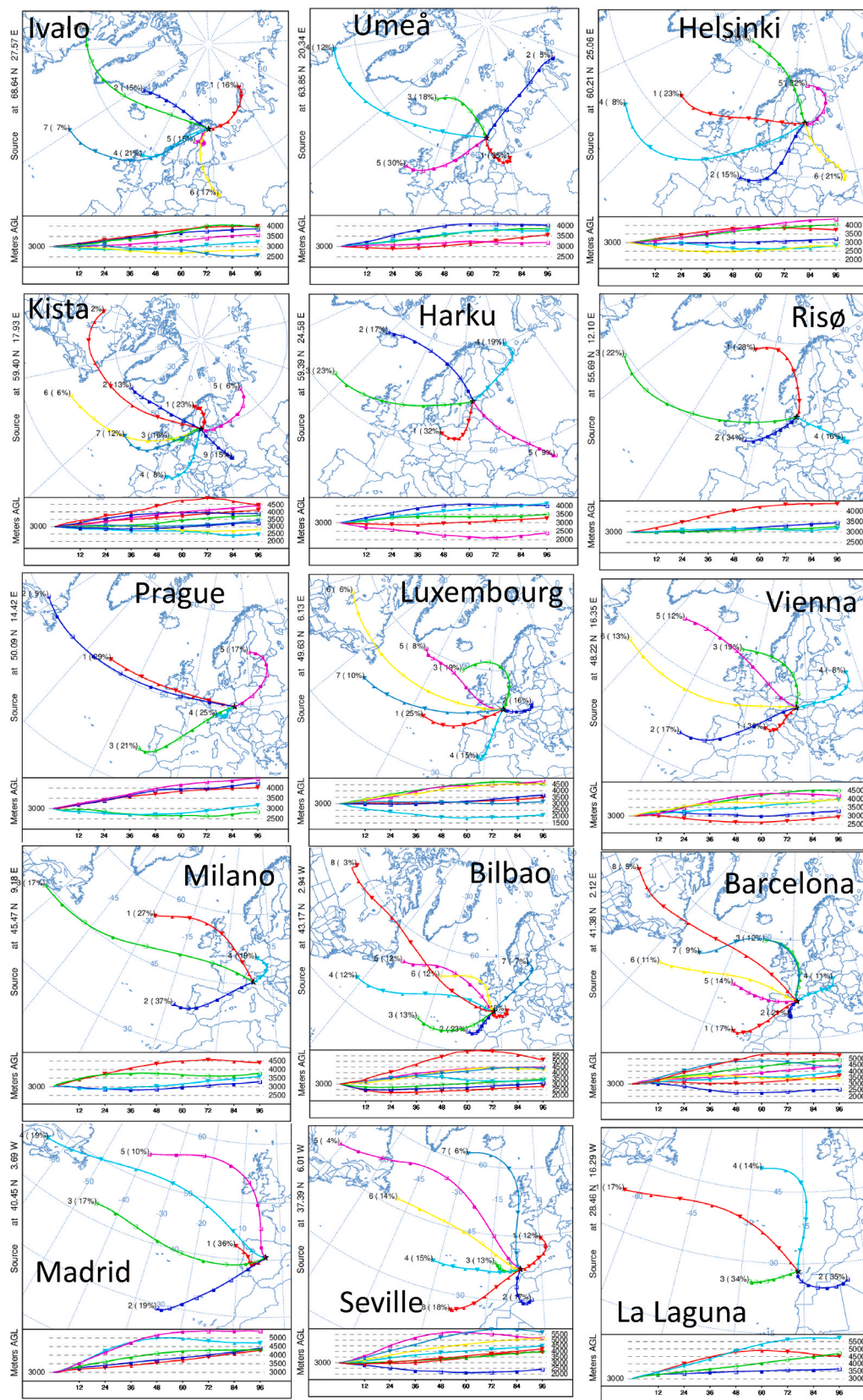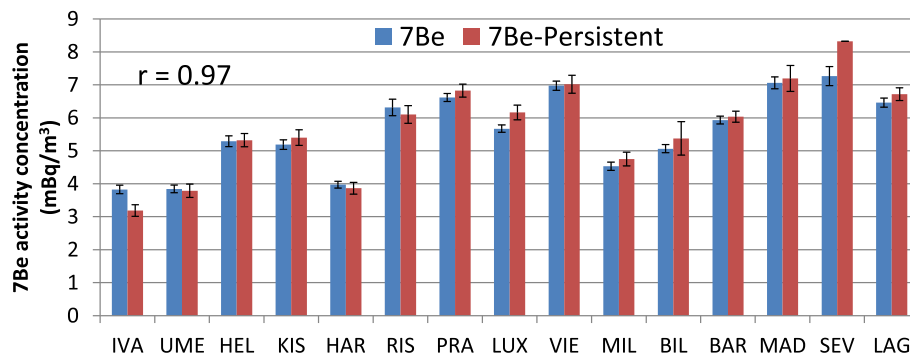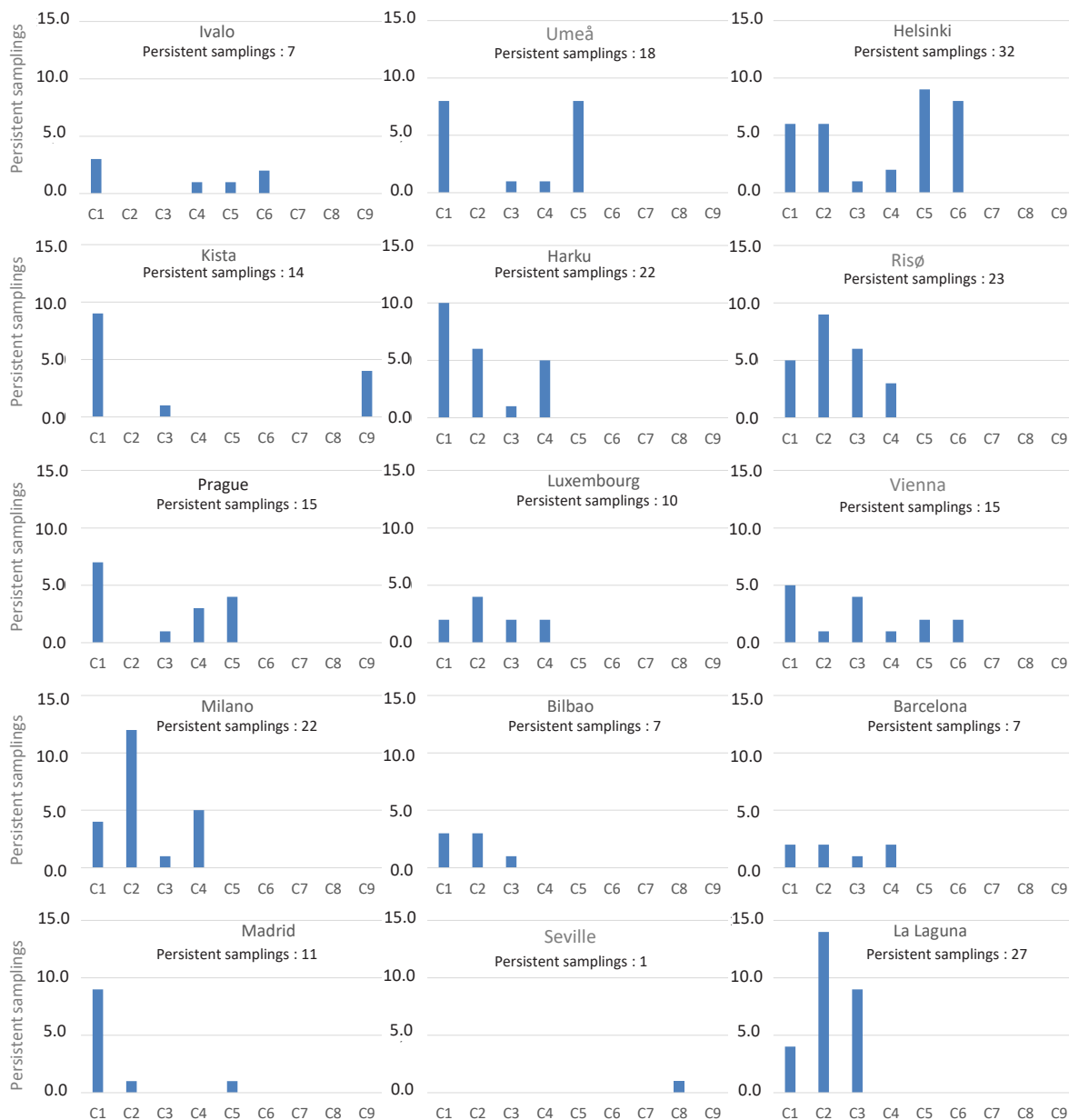

Fig. 4. Seasonal distribution of the extremely high ^{7}Be events over 2005–2014. The stations are ordered by latitude from high to low.

Fig. 5. Average trajectory cluster results (centroids at 3000 m) for the extremely high ^{7}Be values. The stations are ordered by latitude from top to bottom. The numbers on the right in the centroids correspond to the percentage of complete trajectories occurring in that cluster, and the numbers on the left represent an identification for the centroid.

Fig. 6. Comparison of the mean ^{7}Be activity concentration of all the measurements higher or equal P90 (peak ^{7}Be) (blue bar) and the mean of the measurements higher or equal P90 only during the persistent periods (peak ^{7}Be-persistent) (red bar). (For interpretation of the references to colour in this figure legend, the reader is referred to the Web version of this article.)

Fig. 7. Distribution of persistent periods at each station by clusters over 2005–2014. The stations are ordered by latitude from top to bottom.

number of back-trajectory clusters shown in Fig. 5 (9 clusters in Kista). This plot provides a clear representation of the different advection processes and the different influence on the extremely high ^{7}Be activity concentrations in each station. At a first glance, not all nine airflow patterns are associated with persistent sampling periods. Considering the pathways and length of the identified persistent airflow patterns (Fig. 5), they are visually classified into eight advection directions: N, NE, E, SE, S, SW, W, and NW. There is also a pattern identified as Nb which denotes air masses with short pathways and with a center in the vicinity of the sampling station. According to this classification, on average, persistent periods are mainly associated with westerly and easterly advections (46% and 40% of the stations, respectively). Further, south-westerly advections are dominant in five stations (33%), north-easterly in 3 stations (20%), while the rest of possible advections are dominant in only two or one station. No clear spatial distribution of stations emerges according to the most frequent airflow pattern associated with persistent periods. This result clearly suggests again the impact of other factors rather than latitude such as the location of the sampling site and the local atmospheric conditions driving the temporal distribution at one specific station.

Analysing the impact of each airflow pattern on the ^{7}Be peak activity concentrations (not shown) we note that there is a positive and direct influence of the most frequent on registering high activity concentrations. Hence, it is possible to take the most frequent airflow pattern on each station as representative of the synoptic condition associated with the occurrence of the ^{7}Be peak at each specific site. Fig. 8 displays the airflow pathways of those clusters with higher occurrence in connection with the ^{7}Be peak activity concentrations, i.e. those above P90. There are six stations in which the clusters correspond to flows from the east, and in particular NE in Ivalo and Helsinki, E in Luxembourg, and SE in Umeå and La Laguna; in six stations flows originate mostly from the west, such as SW in Risø, Vienna, Milan and Seville, and W in Prague; finally, in the rest of stations the clusters were from the N in Kista, from the S in Harku and Nb in Bilbao, Barcelona and Madrid. In total, there were 105 persistent periods, which mostly occurred during summer (53), followed by spring (28) and autumn (15), and finally winter (5).
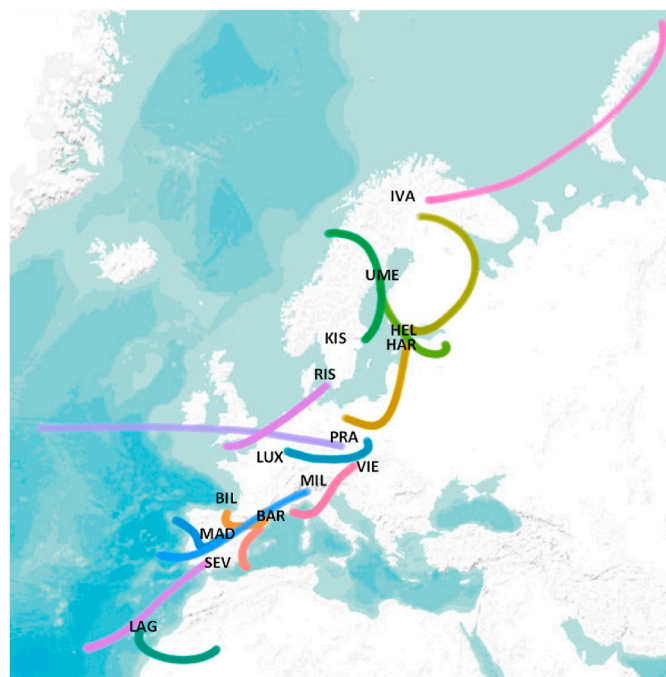

Fig. 8. Airflow patterns more associated with the highest ^{7}Be activity concentrations at each monitoring site (note: Different colours correspond to different sampling sites). (For interpretation of the references to colour in this figure legend, the reader is referred to the Web version of this article.)

Within this variability, it is interesting to note how these patterns present the largest displacement in northern stations, while the displacement gets shorter moving south. These airflow patterns agree with previous studies carried out in different sites (Bilbao, Barcelona, and the Canary Islands) with the purpose to establish a link between the occurrence of ^{7}Be peaks and airflow patterns (Alegría et al., 2020; Grossi et al., 2016; Hernandez et al., 2008). In addition, in the central and northern stations, the concentration of ^{7}Be might increase due to air-mass transport from higher European latitudes, which usually present larger atmospheric ^{7}Be concentrations (e.g., Leppänen et al., 2012; Hernández-Ceballos et al., 2015).

3.3. Synoptic scenarios: teleconnection patterns

Previous sections reported the inter-site variability in the type of airflow pattern with a higher impact on the ^{7}Be activity concentrations across Europe. These patterns also drive the development of mesoscale circulations, and the intensity and variability of local meteorological variables, such as temperature, relative humidity, and precipitation, all of which influence the ^{7}Be activity concentrations. Hence, an in-depth analysis of the synoptic scenarios responsible for the set of airflow patterns identified is needed to understand the occurrence of the ^{7}Be peaks in each site. Large-scale teleconnection patterns, which are usually defined in terms of the height and/or sea level pressure fields, play a key role in determining meteorological conditions and atmospheric circulations over large geographical areas from days to months (Barnston and Livezey, 1987). Taking as reference the set of airflow patterns identified in Fig. 8, and the 105 sampling periods associated, the present section addresses the relationship between them and the five teleconnection patterns: the Arctic Oscillation (AO), North Atlantic Oscillation (NAO), East Atlantic (EA), East Atlantic/West Russia (EAWR), and Scandinavian pattern (SCA) (Lledó et al., 2020). A number of recent analyses have explored a link between the teleconnection patterns and behaviour of the ^{7}Be concentration activity (e.g., Leppänen et al., 2012; Sarvan et al., 2017) and in particular, our previous study on the ^{7}Be peaks in Scandinavia (Ajtić et al., 2018) showed that their occurrence in the autumn/winter period was connected with high values of the Scandinavian pattern. This finding was the basis to further explore a possibility of a similar link in other parts of Europe.

To this purpose, we first need to pay attention to the different temporal coverage of the data, i.e. monthly for most teleconnection indices, and weekly for ^{7}Be activity concentration. This fact limits our ability to establish a direct relationship between them, and to obtain statistically significant results about the influence of each teleconnection index on the airflow patterns, and hence, on ^{7}Be peak concentrations. In addition, the selection of individual persistent periods and the successive identification of airflow patterns with a dominant effect on the ^{7}Be peaks, rule out the possibility to calculate any correlation between both, such as in other studies (e.g. Grossi et al., 2016). So, to investigate a possible influence of each teleconnection index on the ^{7}Be peaks during the dominant airflow pattern, we looked into the corresponding monthly mean indices. More specifically, for each month in which each ^{7}Be peak was registered in each site, we noted the monthly mean value of each teleconnection index and counted the number of peaks observed in the positive and in negative phase.

Fig. 9 represents the number of ^{7}Be peaks associated with positive and negative phases of each index. This analysis points out large variations in the percentage of stations associated with the positive and negative phases of each index. On average, the percentage of stations in the negative phase is higher for the NAO (78%), AO (57%) and EA-WR (57%) indices, while it is only higher for the positive phase of EA (78%). For the SCAND index, there is the same percentage of the stations for the negative and positive phase (42%), while, considering only those stations in the vicinity of the Mediterranean Basin (e.g. Barcelona, Milano, Madrid, Seville), the negative phase of We-MO appears to drive the ^{7}Be peak concentrations. These results suggest that, in general, the ^{7}Be peaks
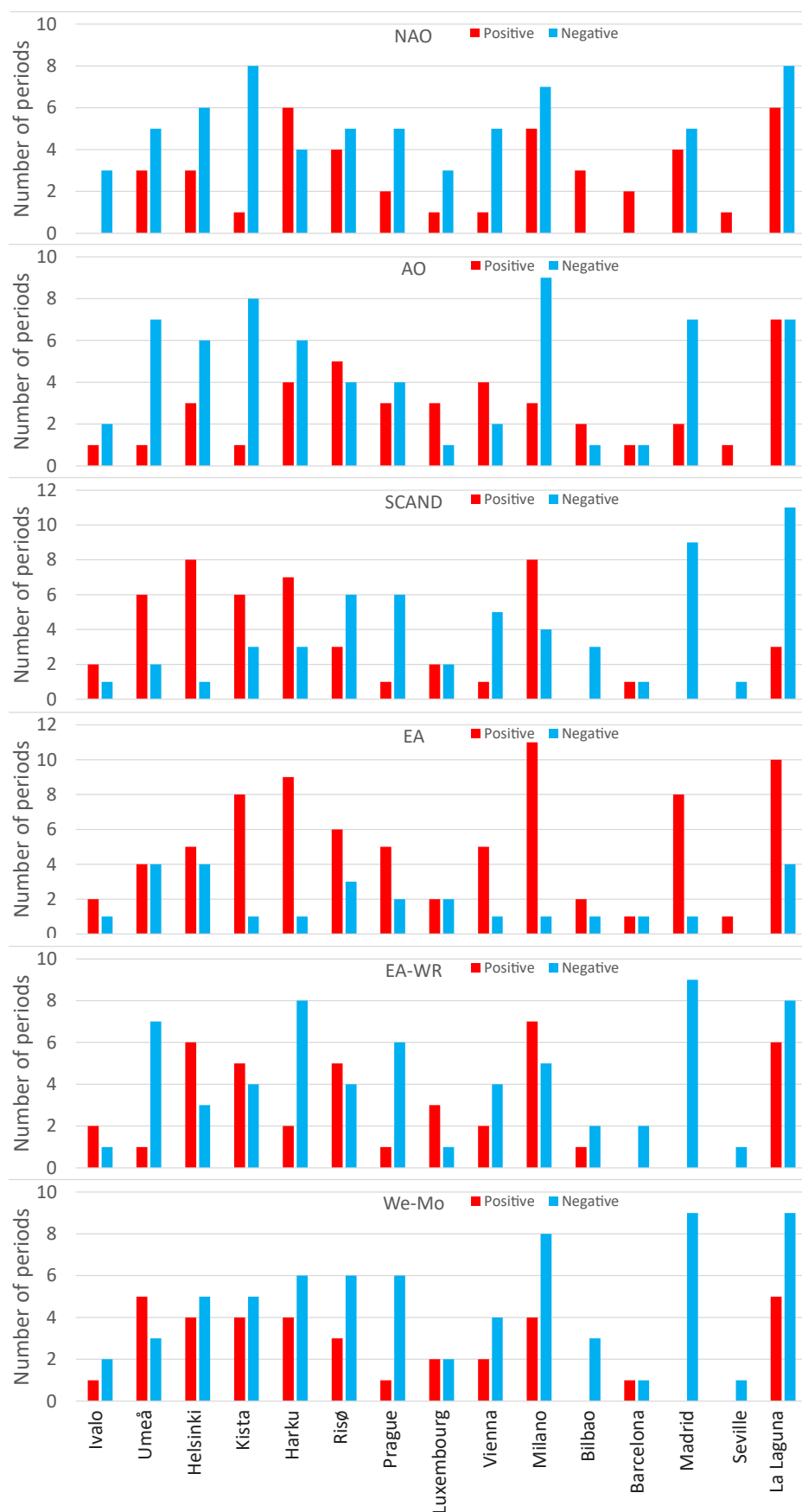
Fig. 9. Number of sampling periods associated with positive and negative phases of each teleconnection index.

across Europe occur mainly during the negative phase of NAO and the positive phase of EA; [7]Be peaks at locations close to the Mediterranean basin are additionally influenced by the negative phase of We-MO. The influence of NAO and EA is justified because they are the two dominant large scale modes over the European region (Hurrell et al., 2002; Athanasiadis et al., 2009). The negative phase of NAO is associated with an atmospheric block with higher than normal heights and atmospheric pressure over Iceland and lower than normal heights and barometric pressure over the Azores, and this synoptic configuration has been previously linked with the occurrence of high [7]Be activity concentrations in many regions of Europe, such as Hernández-Ceballos et al. (2017) in the Iberian Peninsula, and Ajtić et al. (2018) and Brattich et al. (2021) in Scandinavia. In the case of We-MO, Grossi et al. (2014) indicated that the negative phase of this index is generally associated with weakened northerly winds, which can favour an increase in the atmospheric concentrations of [7]Be due to the development of local/mesoscale circulations.

Analysing the results station by station it is possible to identify links between them according to the relationship between [7]Be and the temporal variability of each index. Two groups are clearly identified: 1) Ivalo, Umeå, Helsinki, Kista, Harku and Risø present the same relationship with the following phases of NAO and AO (negative), SCAND and EA (positive), and 2) Bilbao, Barcelona, Madrid, Seville and La Laguna with SCAND and EA-WR (negative) and EA (positive). In the latter, there is also a latitudinal influence as Bilbao and Barcelona, located in the north of the Iberian Peninsula, and Madrid, Seville and La Laguna, located in the south, show the same relationship with the phases of NAO and AO indices, respectively. In this sense, all of these sampling sites present the same behaviour with We-MO. This result may indicate that this index better represents the variability of the cosmogenic radionuclides over southern Europe. The rest of the stations, i.e. Prague, Luxembourg, Vienna and Milan, present similar influences of NAO (negative phase) and EA (positive phase), but with intra-site differences for AO, SCAND and EA-WR. Considering the location of each station, these results could suggest a clear spatial division of stations in two groups, northern and southern, with two additional subgroups; a further group can be distinguished for stations located in the central part of Europe, which present larger variability in the impact of teleconnection patterns.

4. Conclusions

We performed an in-depth analysis of the spatial and temporal variability of the highest [7]Be activity concentrations in the surface air in Europe over 2005–2014, and the synoptic meteorological conditions associated. To this purpose, time series of weekly [7]Be activity concentrations at 15 sampling stations were analysed, as well as clusters analysis of air mass trajectories and indices of the most influencing teleconnection patterns on Europe. The results show a high occurrence of the [7]Be peak concentrations mostly in the spring and summer seasons, and a strong latitudinal impact on the intensity of these peaks. Different types of air masses, both in length and pathway, were found to be associated with the elevated [7]Be concentrations. The present analysis shows that there are specific indices that can support a better understanding of the radionuclide variability, and hence of the main physical processes responsible for its variations, in Europe. Considering the location of each sampling station, the set of the present results reinforces the spatial clusterization of surface [7]Be European stations in two groups, northern and southern. Hence, and for the first time, the variability of different teleconnection indices is found to be linked to the occurrence of the peak [7]Be activity concentrations.

Author statement

Hernández-Ceballos, M.A.: Conceptualization, Methodology, Formal analysis, Writing – original draft. Brattich, E: Methodology, Software,

Visualization, Writing – review & editing. Ajtić, J: Methodology, Visualizacion, Writing – review & editing.

Declaration of competing interest

The authors declare that they have no known competing financial interests or personal relationships that could have appeared to influence the work reported in this paper.

References

Ajtić, J., Brattich, E., Sarvan, D., Djurdjevic, V., Hernández-Ceballos, M.A., 2018. Factors affecting the 7Be surface concentration and its extremely high occurrences over the Scandinavian Peninsula during autumn and winter. Chemosphere 2018 (199), 278–285.

Ajtić, J.V., Sarvan, D., Djurdjevic, V.S., Hernández-Ceballos, M.A., Brattich, E., 2017. Beryllium-7 surface concentration extremes in Europe, facta universitatis – series: Physics. Chem. Technol. 15, 45–55, 2017.

Alegría, N., Hernández-Ceballos, M.A., Herranz, M., Idoeta, R., Legarda, F., 2020. Meteorological factors controlling 7Be activity concentrations in the atmospheric surface layer in northern Spain. Atmosphere 11 (12), 1340.

Athanasiadis, P.J., Wallace, J.M., Wettstein, J.J., 2009. Patterns of jet stream wintertime variability and their relationship to the storm tracks. J. J J Atmos. Sci. 67, 1361–1381.

Brattich, E., Liu, H., Zhang, B., Hernández-Ceballos, M.A., Paatero, J., Sarvan, D., Djurdjevic, V., Tositti, L., Ajtić, J., 2021. Observation and modeling of high-7Be concentration events at the surface in northern Europe associated with the instability of the Arctic polar vortex in early 2003. Atmos. Chem. Phys. 21, 17927–17951.

Barnston, A.G., Livezey, R.E., 1987. Classification, Seasonality and Persistence of Low-Frequency Atmospheric Circulation Patterns. Mon. Weather. Rev. 115, 1083–1126.

Bourcier, L., Masson, O., Laj, P., Pichon, J.M., Paulat, P., Freney, E., Sellegri, K., 2011. Comparative trends and seasonal variation of 7Be, 210Pb and 137Cs at two altitude sites in the central part of France. J. Environ. Radioact. 124, 68–73.

Brattich, E., Liu, H., Tositti, L., Considine, D.B., Crawford, J.H., 2017. Processes controlling the seasonal variations in 210Pb and 7Be at the Mt. Cimone WMO-GAW global station, Italy: a model analysis. Atmos. Chem. Phys. 17, 1061–1080.

Casado, M.J., Pastor, M.A., Doblas-Reyes, F.J., 2008. EuroAtlantic circulation types and modes of variability in winter. Theor. Appl. Climatol. 96, 17–29.

Council of the European Union, 2016. General Secretariat of the Council, the Euratom Treaty : Consolidated Version 2016. Publications Office. https://data.europa.eu/doi/10.2860/45054.

Cristofanelli, P., Bonasoni, P., Tositti, L., Bonafè, U., Calzolari, F., Evangelisti, F., Sandrini, S., Stohl, A., 2006. A 6-year analysis of stratospheric intrusions and their influence on ozone at Mt. Cimone (2165 m above sea level). J. Geophys. Res. Atmos. 111. D03306.

Dorman, L., 2004. Cosmic Rays in the Earth's Atmosphere and Underground. Kluwer Acad., Dordrecht, Netherlands.

Grossi, C., Ballester, J., Serrano, I., Galmarini, S., Camacho, A., et al., 2016. Influence of long-range atmospheric transport pathways and climate teleconnection patterns on the variability of surface 210Pb and 7Be concentrations in southwestern Europe. J. Environ. Radioact. 165, 103–114.

Hernandez, F., Rodríguez, S., Karlsson, L., Alonso-Pérez, S., López-Pérez, M., Hernandez-Armas, J., Cuevas, E., 2008. Origin of observed high 7Be and mineral dust concentrations in ambient air on the Island of Tenerife. Atmos. Environ. 18, 4247–4256.

Hernandez-Ceballos, M.A., Brattich, E., Lozano, R., Cinelli, G., 2017. 7Be behaviour and meteorological conditions associated with 7Be peak events in Spain. J. Environ. Radioact. 166, 17–26.

Hernández-Ceballos, M.A., Cinelli, G., Tollefsen, T., Marín- Ferrer, M., 2016. Identification of airborne radioactive spatial patterns in Europe – feasibility study using Beryllium-7. J. Environ. Radioact. 155–156, 55–62.

Hernández-Ceballos, M. A., Brattich, E., Cinelli, G., Ajtic, J. and Djurdjevic, V.: Seasonality of 7Be concentrations in Europe and influence of tropopause height, Tellus B, 68, 29534.

Huang, S., Huang, P.-H., Newman, S., Li, K.-F., Lin, Y.-C., Huh, C.-A., Lin, N.-H., Hsu, S.-C., Liang, M.-C., 2022. Enhanced stratospheric intrusion at Lulin Mountain, Taiwan inferred from beryllium-7 activity. Atmos. Environ. 268, 118824.

Hurrell, J.W., Kushnir, Y., Ottersen, G., Visbeck, M., 2002. An overview of the north Atlantic oscillation. In: The North Atlantic Oscillation−Climate Significance and Environmental Impact, Geophys. Monogr, vol. 134. American Geophysical Union, pp. 1–35.

Ioannidou, A., Papastefanou, C., 2006. Precipitation scavenging of 7Be and 137Cs radionuclides in air. J. Environ. Radioact. 85, 121–136.

Ioannidou, A., Eleftheriadis, K., Gini, M., Gini, L., Manenti, S., Groppi, F., 2019. Activity size distribution of radioactive nuclide 7Be at different locations and under different meteorological conditions. Atmos. Environ. 212, 272–280.

Kusmierczyk-Michulec, J., Gheddou, A., Nikkinen, M.T., 2015. Influence of precipitation on 7Be concentrations in air as measured by CTBTO global monitoring system. J. Environ. Radioact. 144, 140–151.

Lee, H.N., Tositti, L., Zheng, X., Bonasoni, P., 2007. Analyses and comparisons of variations of 7 Be, 210Pb, and 7 Be/210 666 Pb with ozone observations at two Global Atmosphere Watch stations from high 667 mountains. J. Geophys. Res. 112. D05303.

Leppänen, A.-P., Usoskin, I.G., Kovaltsov, G.A., Paatero, J., 2012. Cosmogenic 7 Be and 22Na in Finland: production, observed periodicities and the connection to climatic phenomena J. Atmos. Sol.-Terr. Phys. 74, 164–180.

Lledó, L., Cionni, C., Torralba, V., Bretonnière, P.A., Samsó, M., 2020. Seasonal prediction of Euro-Atlantic teleconnections from multiple systems. Environ. Res. Lett. 15 (7).

Lozano, R.L., San Miguel, E., Bolívar, J.P., Baskaran, M., 2011. Depositional fluxes and concentrations of 7Be and 210Pb in bulk precipitation and aerosols at the interface of Atlantic and Mediterranean coasts in Spain. J. Geophys. Res. 116 (D18).

Martin-Vide, J., Lopez-Bustins, J.A., 2006. The western Mediterranean oscillation and rainfall in the Iberian Peninsula. Int. J. Climatol. 26, 1455–1475.

McNeary, D., Baskaran, M., 2003. Depositional characteristics of 7Be and 210Pb in southeastern Michigan. J. Geophys. Res. 108 (D7).

Pacini, A.A., Usoskin, I.G., Mursula, K., Echer, E., Evangelista, H., 2015. Signature of a sudden stratospheric warming in the near-ground 7 Be flux. Atmos. Environ. 113, 27–31.

Persson, B.R., 2016. Global distribution of 7Be, 210Pb and, 210Po in the surface air (with Appendix A-E). Acta Scientiarum Lundensia 001, 1–51. Bertil RR Persson, Medical Radiation Physics, 22185.

Rolph, G., Stein, A., Stunder, B., 2017. Real-time environmental applications and display sYstem: READY. Environ. Model. Software 95, 210–228.

Sangiorgi, M., Hernández Ceballos, M.A., Iurlaro, G., Cinelli, G., de Cort, M., 2019. 30 years of European Commission Radioactivity Environmental Monitoring Database (REMdb) – an open door to boost environmental radioactivity research. Earth Syst. Sci. Data 11, 589–601.

Sarvan, D., Stratimirovic, D., Blesic, S., Djurdjevic, V., Miljkovic, V., Ajtic, J., 2017. Dynamics of beryllium-7 specific activity in relation to meteorological variables, tropopause height, teleconnection indices and sunspot number. Phys. A: Stat. Mech. Appl. 469, 813–823.

Stein, A.F., Draxler, R.R., Rolph, G.D., Stunder, B.J.B., Cohen, M.D., Ngan, F., 2015. NOAA's HYSPLIT atmospheric transport and dispersion modeling system. Bull. Am. Meteorol. Soc. 96, 2059–2077.

Steinmann, P., Zeller, M., Beuret, P., Ferreri, G., Estier, S., 2013. 2013. Cosmogenic 7Be and 22Na in ground level air in Switzerland (1994-2011). J. Environ. Radioact. 124, 68–73.

Stunder, B.J.B., 1996. An assessment of the quality of forecast trajectories. J. Appl. Meteorol. Climatol. 35, 1319–1331.

Talpos, S., Cuculeanu, V., 1997. A study of the vertical diffusion of 7Be in the atmosphere. J. Environ. Radioact. 36, 93–106.

Terzi, L., Kalinowski, M.B., 2017. World-wide seasonal variation of 7Be related to large-scale atmospheric circulation dynamics. J. Environ. Radioact. 179, 1–15.

Yoshimori, M., 2005. Production and behavior of beryllium 7 radionuclide in the upper atmosphere. Adv. Space Res. 36, 922–926.